

# Supplementary material for *Approximating Matsubara dynamics using the planetary model: tests on liquid water and ice*

Michael J. Willatt, Michele Ceriotti and Stuart C. Althorpe

## Computational details for the calculation of infrared absorption spectra

### Gas-phase simulations

To calculate the quantum results in this study, we implemented the q-TIP4P/F potential and dipole moment surface<sup>1</sup> into the DVR3D package of Tennyson et al.<sup>2</sup> This package computes the energy levels of the system and the matrix elements of the dipole moment operator in the basis of eigenstates. We combined these to compute the real part of the standard quantum dipole moment autocorrelation function. To simulate the effect of quantum decoherence, we applied a Hann window to the quantum autocorrelation function before taking its Fourier transform. The Hann window is given by<sup>3</sup>

$$w(t; \Delta t) = \begin{cases} \frac{1}{2} (\cos(\pi t / \Delta t) + 1) & |t| \leq \Delta t \\ 0 & \text{elsewhere} \end{cases} \quad (\text{S1})$$

At each temperature, we chose the parameter  $\Delta t$  to be commensurate with the time taken for the TRPMD dipole moment autocorrelation function to decorrelate ( $\Delta t = 500$  fs (150K), 400 fs (300K) and 300 fs (600K)). The Fourier-transformed result was then inserted into Eq. (48) with an arbitrary volume to produce the infrared absorption spectrum. The effect of the Hann window on the quantum infrared absorption spectrum at 300K is shown in Fig. S1.

To calculate the classical and TRPMD results, we calculated each dipole moment autocorrelation over a total of  $10^6$  independent trajectories of length 2 ps. These were then treated using the same Hann window as for the quantum results before taking their Fourier transforms. To ensure independence of trajectories for the classical simulations we employed an Andersen thermostat to resample momenta.<sup>4</sup> We used a time step of  $\Delta t = 0.25$  fs for both methods with a symmetric velocity Verlet algorithm (classical) and the algorithm described in ref. 5 to integrate the TRPMD equations of motion. To converge the TRPMD results with respect to the number of ring-polymer beads we used  $N = 64$  (150K), 32 (300K) and 16 (600K).

To calculate the planetary model results, we used the same TRPMD code with a symmetric velocity Verlet algorithm for alternating propagation of the centroids and planets

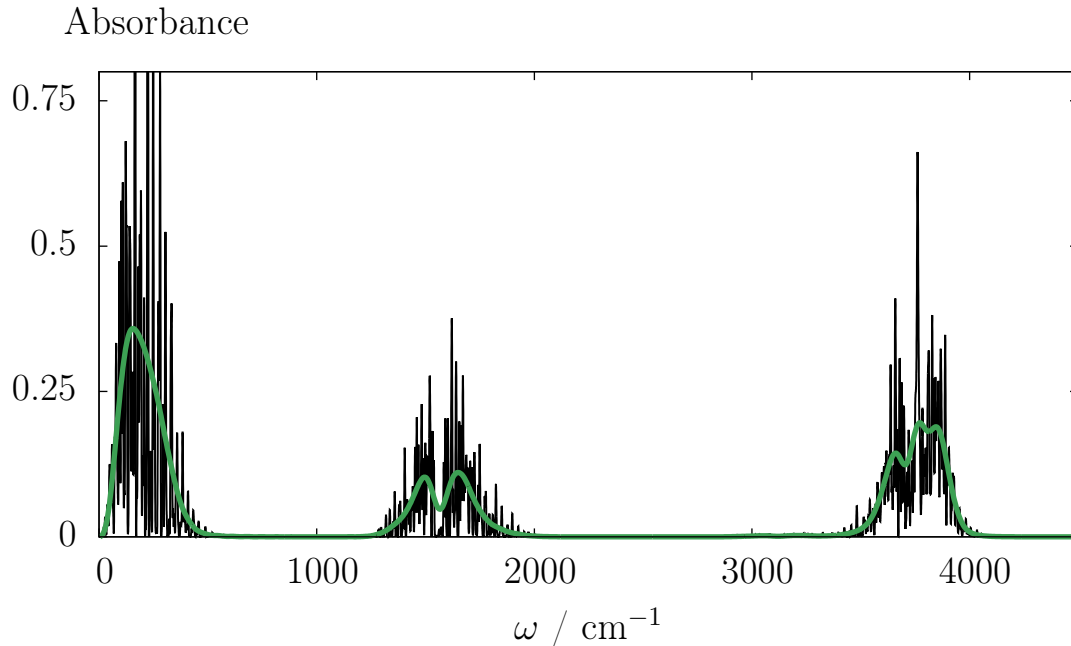


Figure S1: Infrared absorption spectra for the q-TIP4P/F water molecule at 300K. The absorbance is given in arbitrary units. The black and green lines show the infrared absorption spectra with the use of the Hann window (green) and without (black).

with a time step of  $\Delta t = 0.25$  fs and set any instantaneous imaginary eigenfrequencies to zero. At each temperature we used the same number of ring polymer beads as mentioned previously for the TRPMD simulations. To calculate the approximate FK effective frequency matrix Eq. (40), we spawned an independent TRPMD centroid-constrained trajectory of length 64 fs at each time step and calculated the thermal average as a time average along the trajectory. We used a total of 64 independent initial planet phase space points (drawn from the relevant normal distribution:  $\bar{q}_j, \bar{p}_j \sim \mathcal{N}(0, 1)$  for  $j = 1, 2, \dots, D$ ) to converge the integrals over the distribution of the planets. We calculated the dipole moment autocorrelation over a total of  $10^4$  independent centroid trajectories of length 2 ps (one for each of the 64 initial positions and momenta of the planets). The aforementioned Hann window and Fourier transform procedure was then used for each autocorrelation function to generate the infrared absorption spectra.

## Condensed-phase simulations

We used the i-PI package of Ceriotti et al.<sup>6</sup> (including the packaged q-TIP4P/F driver) to calculate the classical, TRPMD and planetary model infrared absorption spectra of q-TIP4P/F water in the condensed phase. We simulated hexagonal ice at 150K, liquid at 300K and (compressed) liquid at 600K under periodic boundary conditions. Our simulation box consisted of 96 water molecules for hexagonal ice and 128 water molecules for the liquid at 300K and 600K. These are the same thermodynamic conditions as were used by Rossi et al. in ref. 7. To determine the size of the simulation box we used the

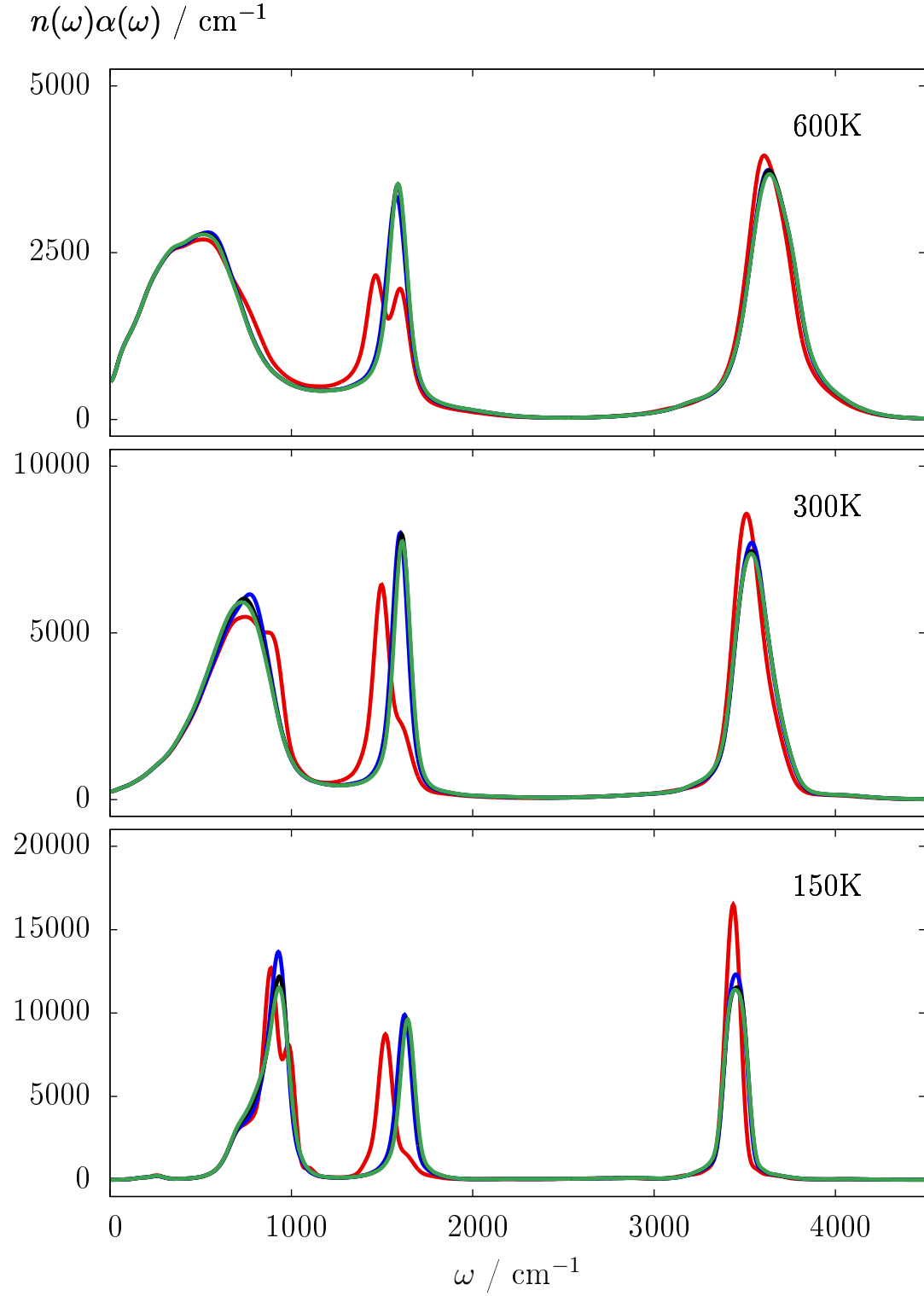


Figure S2: Convergence of the planetary model infrared absorption spectra with respect to the screening matrix parameter  $\gamma$  in Eq. (S3). The lines correspond to  $\gamma = 0.25$  (red), 0.13 (blue), 0.10 (black) and 0.09 (green) in  $\text{a.u.}^{-1}$ .

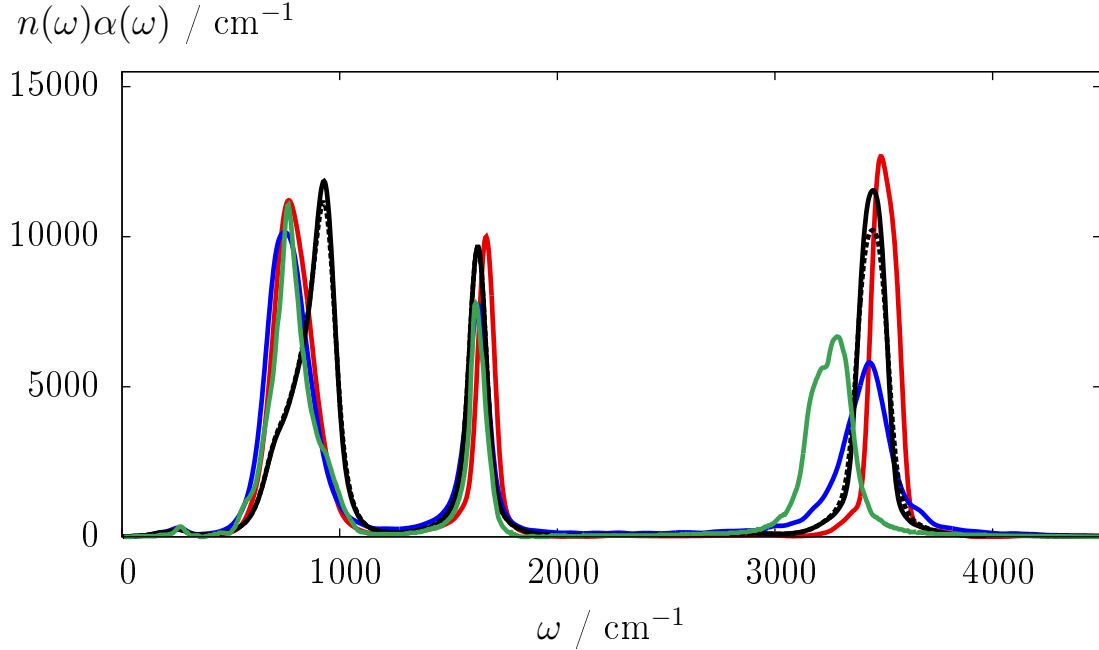


Figure S3: The effect of using RPMD instead of TRPMD to calculate the planetary part of the infrared absorption spectrum for q-TIP4P/F hexagonal ice at 150K. The lines correspond to classical (red), TRPMD (blue), CMD (green), the planetary model (solid black) and the planetary model with RPMD instead of TRPMD for evolution of  $\Omega(\mathbf{Q}_{0,t})$  (dashed black).

experimental density of hexagonal ice and the liquids at the relevant temperatures, which at 600K was the density of the liquid at the liquid-vapour coexistence point. To generate initial hexagonal ice geometries at 150K we used the Monte Carlo procedure described in ref. 8 to ensure consistency with the Bernal-Fowler rules<sup>9</sup> which were then evolved under thermostatted ring-polymer or classical (Andersen-thermostatted) dynamics. The initial liquid configurations were generated straightforwardly using only the thermostatted ring-polymer or classical dynamics.

We used a time step of  $\Delta t = 0.25$  fs for all the simulations and  $N = 64$  (150K), 32 (300K) and 16 (600K) ring-polymer beads for the TRPMD and planetary model simulations in accordance with the previous study by Rossi et al.<sup>7</sup> For the classical and TRPMD simulations we calculated the autocorrelation of the total dipole moment derivative of the simulation box over 256 independent trajectories of length 10 ps. We then applied the aforementioned Hann window and Fourier transform procedure ( $\Delta t = 500$  fs) to the autocorrelation functions to generate the infrared absorption spectra, making use of the following relation,

$$\tilde{G}_{\dot{\mu}\dot{\mu}}(\omega) = \omega^2 \tilde{G}_{\mu\mu}(\omega). \quad (\text{S2})$$

There are three important computational differences between how we calculated the planetary model infrared absorption spectra for the gas phase and the condensed phase. First, we found that we need not calculate the approximate FK effective frequency matrix every

0.25 fs, but could rather calculate it every 1 fs and use linear interpolation to approximate the intervening matrices without any loss in quality of the resulting infrared absorption spectra. Second, we took the Hadamard product of the approximate FK effective frequency matrix with the following screening matrix,

$$S_{ab} = \exp(-\gamma^2 r_{ab}^2), \quad (\text{S3})$$

where  $\gamma$  is an adjustable parameter and  $r_{ab}$  is the distance between the centroids that pertain to the  $a^{\text{th}}$  and  $b^{\text{th}}$  dimensions. We found that a value of  $\gamma = 0.10 \text{ a.u.}^{-1}$  was sufficient to give the same result as with a smaller value but without the expense of significantly longer centroid-constrained TRPMD trajectories (see Fig. S2). With this modification we were able to use centroid-constrained TRPMD trajectories of length 128 fs. Third, we exploited the different convergence properties of the TRPMD and planetary (fluctuation) contributions to the infrared absorption spectra by calculating each part in a separate simulation. We have already described the calculation of the TRPMD part, while for the planetary part we found we obtained a converged result by correlating the total dipole moment of the simulation box (evaluated at  $\tilde{\mathbf{q}}$ ) over only 8 trajectories of length 2 ps at each temperature. As for the gas-phase simulations, we used a total of 64 independent initial planet phase space points to converge the integrals over the phase space distribution of the planets. The aforementioned Hann window and Fourier transform procedure ( $\Delta t = 500 \text{ fs}$ ) was then applied to these autocorrelation functions to generate the planetary contributions to the infrared absorption spectra.

## The effect of using RPMD instead of TRPMD to evolve the time-dependent frequency matrix $\Omega(\mathbf{Q}_{0,t})$

To assess the importance of the choice of centroid dynamics for the planetary part of the q-TIP4P/F infrared absorption spectra, we repeated our hexagonal ice simulations with RPMD evolution of  $\Omega(\mathbf{Q}_{0,t})$  instead of TRPMD. The effect is shown in Fig. S3. The libration and stretch bands are slightly broadened and diminished by this change, while the bend band is unaffected to graphical accuracy. This helps to justify our speculation that CMD, RPMD and TRPMD will provide a very similar description of fluctuation dynamics when used with the planetary model, at least for observables that are linear in the position operator.

## References

- [1] S. Habershon, T. E. Markland, and D. E. Manolopoulos, *J. Chem. Phys.* **131**, 024501 (2009).
- [2] J. Tennyson et al., *Comput. Phys. Commun.* **163**, 85 (2004).
- [3] F. Harris, *Proc. IEEE* **66**, 51 (1978).
- [4] H. C. Andersen, *J. Chem. Phys.* **72**, 2384 (1980).
- [5] M. Rossi, M. Ceriotti, and D. E. Manolopoulos, *J. Chem. Phys.* **140**, 234116 (2014).
- [6] M. Ceriotti, J. More, and D. E. Manolopoulos, *Comput. Phys. Commun.* **185**, 1019 (2014).

- [7] M. Rossi, H. Liu, F. Paesani, J. Bowman, and M. Ceriotti, *J. Chem. Phys.* **141**, 181101 (2014).
- [8] V. Buch, P. Sandler, and J. Sadlej, *J. Phys. Chem. B* **102**, 8641 (1998).
- [9] J. D. Bernal and R. H. Fowler, *J. Chem. Phys.* **1**, 515 (1933).